Montserrat Hernández-Alamilla and Alex Valadez-Gonzalez*

The effect of two commercial melt strength enhancer additives on the thermal, rheological and morphological properties of polylactide

Abstract: The effect of two commercial melt strength enhancer additives, Paraloid BPMS-250 (BPMS) and Biostrength 700 (BIOS), on the thermal, rheological and morphological properties of polylactide (PLA) was studied. Thermal analyses showed that both the BPMS and BIOS additives decreased the ability of PLA to crystallize. The rheological tests indicated that zero-shear viscosity and storage modulus of the PLA/BPMS and PLA/BIOS blends were significantly increased with the additive content. These could be attributed to the entanglements between the PLA chains with those of the high molecular weight additive, creating a physical network which reduces the segmental mobility of PLA and improves the melt elasticity of the blend. The entanglement molecular weights (M)of PLA/BPMS and PLA/BIOS blends were lower than those of unprocessed and processed PLA ($M_a \approx 4 \times 10^4$ g/mol), which suggests greater chain entanglements and a higher entanglement density (v_s) . The elongational viscosity (η_s) and melt strength values were estimated using a screwextrusion capillary rheometer, where the PLA/BIOS blends presented the highest values. Finally, scanning electron microscopy on the samples was carried out to assess the blend morphology.

Keywords: melt elasticity; melt strength enhancer; polylactide.

DOI 10.1515/polyeng-2014-0322 Received November 1, 2014; accepted April 2, 2015; previously published online May 14, 2015

Montserrat Hernández-Alamilla: Unidad de Materiales, Centro de Investigación Científica de Yucatán A.C. 130 No. 43 Chuburná de Hidalgo, 97200, Mérida Yucatán, Mexico

1 Introduction

In recent years one of the trends in the polymer field has been the replacement of traditional petroleum-derived plastics with biodegradable ones in order to diminish the waste disposal problems [1]. Polylactide (PLA) is a thermoplastic aliphatic polymer compostable and renewable [2]. It is a biocompatible [3] and economical material, compared with other biodegradable polymers, and its physical and mechanical properties are comparable to those of many petroleum-derived plastics [4]. However, PLA does not offer the processability needed for applications where stretching or drawing is involved like melt spinning, blow molding and blown film extrusion, due to its poor melt stability and low melt strength [5, 6]. The low melt strength of PLA, which is directly associated with its linear chain structure, tends to cause sagging and necking, reducing the processing throughput [7]. Moreover, during processing, the chain scission, due to hydrolysis and thermal instability, and the lactide formation by the back-biting mechanism, cause loss of molecular weight and viscosity [8–11]. The melt strength of a polymer is a measure of its resistance to extensional deformation and it is related to the molecular chain entanglements of the polymer and its resistance to untangling under strain. Recent studies describe the use of a single-screw extruder equipped with a capillary die and a Göttfert Rheotens melt strength tester [12-14] to measure out the plastics melt strength. The properties affecting the resistance to untangling are molecular weight, molecular weight distribution and molecular chain entanglements or branching of the polymer. As each property increases, the melt strength improves [15]. PLA needs to be melt-strengthened in order to enlarge its processing window and its range of applications. Many methods have been reported, such as increasing the molecular weight, broadening the relative molecular weight distribution, changing the molecular structure, the filling modification and blending modification [16]. Södergard and Stolt [17] presented a method to stabilize PLA using an organic peroxy compound (e.g., tert-butyl peroxybenzoate, dibenzoyl peroxide, tert-butyl peroxyacetate). Carlson et al. [18, 19] modified PLA using

^{*}Corresponding author: Alex Valadez-Gonzalez, Unidad de Materiales, Centro de Investigación Científica de Yucatán A.C. 130 No. 43 Chuburná de Hidalgo, 97200, Mérida Yucatán, Mexico, e-mail: avaladez@cicy.mx

maleic anhydride and a range of alkoxy forming peroxides. Zhou et al. [20] obtained a copolymer prepared by chain extension of dicarboxylated PLLA and a diglycidyl ether of bisphenol-A (DGBA) based epoxy resin. Najafi et al. [21] prepared PLA-clay nanocomposites using polycarbodiimide, tris(nonyl phenyl) phosphate and Joncryl ADR-4368 as chain extenders. Liu et al. [16], Corre et al. [22], Mihai et al. [23] and Pilla et al. [24], employed a multi-functional epoxy-based chain extender (Cesa-Extend from Clariant) to give rise to branched structures of PLA. Recently, Han et al. [25] used polysilsesquioxane microspheres as novel chain extenders to improve the thermal stability of PLA. PLA has also been blended with different plasticizers, additives and/or polymers to improve desired properties [26–30]. Acrylic-based additives, so-called melt strength enhancers, have been designed to improve the melt strength and hence, the processability of PLA and its alloys. When added at levels as low as 2 wt% during thermal processing, it increases the melt elasticity of the blend. These additives protect the PLA from degradation and help the polymer chains to attenuate the loss of molecular weight and viscosity of the melt [31]. The entanglement of PLA chains with those of the high molecular weight acrylic creates a physical network with a high resistance to break in the melt [32]. However, to our knowledge there are no reports in the literature related with the incorporation of melt-strengthening commercial additives to PLA. The aim of this work was to assess the effect of the incorporation of two commercial melt strength enhancer additives on the thermal, rheological and morphological properties of PLA.

2 Materials and methods

2.1 Materials

NatureWorks (Minnetonka, MN, USA) semicrystalline PLA 4032D-grade comprising around 2% of D-lactic acid monomer was used (Table 1). It can be converted into a biaxially oriented film. The film has excellent optical properties, good machinability, excellent twist and dead

Table 1: Properties of polylactide (PLA) 4032 D.

Material	M _W ^a (g/mol)	M _n ^a (g/mol)	MFl ^b (g/10 min)	
Unprocessed	164,840	90,280	8.7	
Processed	112,545	61,122	25.4	

^aDetermined by gel permeation chromatography (GPC).

fold properties and acts as a good barrier to flavor and grease and oil resistance [33]. The melt strength enhancer additives were Paraloid BPMS-250 (BPMS) provided by the Rhom and Haas Company (Philadelphia, PA, USA) [32] and Biostrength 700 (BIOS) from Arkema Inc. (King of Prussia, PA, USA) [34] derived from natural renewable sources. Typical properties are shown in Table 2. The formulation is proprietary; however, both additives are acrylic copolymers that have 60% or more of acrylic and/or methacrylic monomer units where acrylic monomers include methacrylates and/or acrylates. In addition, the acrylic copolymer can also include up to 40% of other ethylenically unsaturated monomers polymerizable with the acrylic monomers including, styrene, alpha-methyl styrene, vinyl acetate, vinylidene fluorides, vinylidene chlorides, acrylonitrile, vinyl sulfone, vinyl sulfides and vinyl sulfoxides [35]. All materials were dried overnight in a vacuum oven at 60°C before processing to remove moisture.

2.2 Blend preparation

PLA pellets were ground using a Brabender laboratory mill (Duisburg, Germany) into 1 mm particles before blending to make dispersion better. Table 3 summarizes the mixing composition of the PLA/BPMS and PLA/BIOS blends. Primarily, PLA and the melt strength enhancer were premixed by hand in a plastic container. Then, PLA blends were prepared by melt blended using a Brabender counter-rotating conical twin-screw extruder (Model CTSE-V, S. Hackensack, NJ, USA) with approximately 30:1 L/D ratio. The temperature profile along the extruder barrel was set at 165°C-175°C-180°C and 175°C (from feed zone to die), controlled with a Brabender temperature control console (Model 808-2503, S. Hackensack, NJ, USA). The screw speed was 40 rpm. The extruded strands were cut in a 2" Brabender laboratory pelletizer (Model 12-72-000, S. Hackensack, NJ, USA). Finally, the pellets were conditioned for 4 h at 80°C under vacuum and kept sealed until ready to use.

Table 2: Typical properties of melt strength enhancer additives.

	Paraloid™ BPMS-250	Biostrength® 700
Physical form	White powder	White powder
Specific gravity	1.19	1.17
Bulk density	0.4-0.52 g/ml	0.45 g/ml
Particle size	_	2% Maximum on 40 mesh
Percent volatiles	_	1.2% Maximum
Melting point/range	132-149°C	_
Water solubility	Insoluble	Insoluble

^bDetermined by melt flow indexer at 190°C and 2160 g.

Table 3: Designations and compositions of polylactide (PLA)/melt strength enhancer blends.

Sample	PLA (wt%)	Paraloid™ BPMS- 250 (wt%)	Biostrength® 700 (wt%)	
Processed PLA ^a	100.0	0	0	
PLA/BPMS-2	98.0	2.0	0	
PLA/BPMS-5	95.0	5.0	0	
PLA/BPMS-10	90.0	10.0	0	
PLA/BIOS-2	98.0	0	2.0	
PLA/BIOS-5	95.0	0	5.0	
PLA/BIOS-10	90.0	0	10.0	

^aExtruded PLA without melt strength enhancer additive.

2.3 Determination of thermal properties

The thermal properties were determined by differential scanning calorimetry (DSC) on a PerkinElmer Pyris Diamond DSC (Waltham, MA, USA) under a nitrogen atmosphere at a flow rate of 20 ml/min. In order to eliminate the influence of thermal history, all samples (about 5–8 mg sealed in aluminum pans) were first heated from room temperature up to 190°C and held at that temperature for 5 min, then cooled down to 45°C (i.e., 1st cooling) to record the crystallization temperature and finally heated again (i.e., 2nd heating). All the scanning rates for the DSC measurements were held at 10°C/min. Two repetitions were made for each formulation to ensure repeatability. Temperatures and enthalpies at glass transition, crystallization and melting were determined. The glass transition temperature (T_a) was recorded as the midpoint of the heat capacity change during the transition. The melting temperature $(T_{...})$ was recorded at the maximum of the enthalpy peak corresponding to the melting (ΔH_m) . The degree of crystallinity of the samples (X_{\cdot}) was estimated from the heat evolved during crystallization according to the following equation:

$$X_{c}(\%) = \frac{\Delta H_{m} - \Delta H_{cc}}{\varnothing_{\text{PI} \Delta} \Delta H_{m}^{0}} \times 100$$
 (1)

where ΔH_m , ΔH_{cc} and ΔH_m^o (J/g) are enthalpies of fusion, cold crystallization and for 100% crystalline PLA, respectively; \emptyset_{PLA} is the weight fraction of PLA in blends. The heat of fusion for pure PLA crystal (100% crystallinity) used was 93.6 J/g [36].

2.4 Determination of rheological properties

The melt flow index (g/10 min) was measured, using a Kayeness Galaxy I melt flow indexer (Model D7053, Morgantown, PA, USA) at standard conditions of 190°C under a load of 2160 g in accordance with ASTM D-1238 [37]. The reported melt index is an average of five samples. The dynamic oscillatory measurements were carried out on a rotational AR-2000 rheometer (TA Instruments, New Castle, DE, USA), equipped with parallel plates geometry, at 180°C. Primarily, sheets of all samples were prepared by compression molding at 170°C using a Carver hot press (Model 3891.4DI1A00, Wabash, IN, USA). Then, the compression molded samples of 1.0±0.1 mm thick were cooled to room temperature under ambient conditions and cut into 25 mm diameter discs. Frequency sweeps were carried out over an angular frequency ranging from 0.1 to 600 rad/s at a fixed strain of 10%. The gap distance between the parallel plates was 0.8 mm for all tests. The linear viscoelastic region was initially confirmed from a strain sweep test. Special care was taken to dry the samples for 24 h in a vacuum oven at 60°C prior to the rheological testing in order to avoid a significant decrease in viscosity. At least three repetitions of each dried formulation were made to ensure repeatability. The elongational viscosity was estimated from the Cogswell converging flow model [38]. The rheological properties necessary for the application of the model were measured by the screw-extrusion capillary rheometer in accordance with ASTM D-5422 [39] using a single-screw Brabender extruder (Model CTSE-V, S. Hackensack, NJ, USA) with 24:1 L/D ratio. The temperature profile was set at 160°C–170°C– 180°C and 175°C at the die. The output end of the extruder was equipped with a capillary die (using the 2.0 mm insert series with 10, 15 and 20 L/D ratios), pressure transducer and a temperature sensor. The material was extruded through the capillary (for each insert) at different screw speeds from 15 to 60 rpm with increments of 15. The volumetric flow rate (Q) was calculated by weighing material collected over 2 min. A constant density of 1.12 g/cm³ was assumed. Each experiment was repeated in triplicate. The apparent shear viscosity η (Pa·s) was calculated using the following equations:

$$\tau_{w} = \frac{P}{4\left[(L/D) + E \right]} \tag{2}$$

$$\dot{\gamma}_{w} = \left[\frac{3n+1}{4n}\right] \dot{\gamma}_{a} \tag{3}$$

$$\eta = \frac{\tau_{w}}{\dot{\gamma}_{w}} \tag{4}$$

where τ_{w} is the corrected shear stress (Pa), $\dot{\gamma}_{w}$ is the corrected shear rate (s⁻¹), P is the pressure at the entrance of the capillary (Pa), L is the length of the capillary (mm), D is the diameter of the capillary (mm), E is the Bagley correction factor (dimensionless), n is the shear sensitivity (dimensionless) and $\dot{\gamma}_a = 32 \cdot Q / \pi \cdot D^3$ is the apparent shear rate (s¹). Assuming that the dependence of the shear viscosity (η) on the shear rate ($\dot{\gamma}_w$) is described by a power-law relationship and that the elongational viscosity is independent of the strain rate, the elongational viscosity and the corresponding elongational rate can be calculated as:

$$\dot{\varepsilon} = \frac{4}{3} \frac{\eta}{(n+1)} \frac{\dot{\gamma}_w}{\Delta P_0} \tag{9}$$

$$\sigma_E = \frac{3}{8} (n+1) \Delta P_0 \tag{6}$$

$$\eta_E = \frac{\sigma_E}{\dot{\varepsilon}} = \frac{9}{32} \frac{\left(n+1\right)^2}{\eta} \left(\frac{\Delta P_0}{\dot{\gamma}_w}\right)^2 \tag{7}$$

where η_E is the elongation viscosity (Pa·s), σ_E is the elongation stress (Pa), $\dot{\varepsilon}$ is the elongation rate (s¹), ΔP_0 is the capillary drop pressure (Pa) and η is the apparent shear viscosity obtained with Bagley correction (Pa·s). The melt strength was estimated using the methodology proposed by Morris and Bradley [40]. The blends were dried overnight in a vacuum oven at 60°C and then they were extruded at a screw speed of 30 rpm using a 2.0 mm diameter and L/D=20 capillary die. Around 200 mm of filament length was extruded in about 100 s and the melt strength was estimated as the ratio of the capillary/strand diameter; the latter was measured at a distance of 80 mm over the end of the extrudate.

2.5 Blend morphology

The morphology of the fracture surface of pure PLA and PLA/additive blends were characterized using a JEOL scanning electron microscope (SEM model JSM-6360LV, Peabody, MA, USA). The sample sheets were fractured after freezing in liquid nitrogen and sputter-coated uniformly with gold over all the fractured surfaces to enhance the conductivity prior to the SEM observations at an accelerating voltage of 20 kV.

3 Results and discussion

3.1 Thermal properties analysis

DSC measurements were conducted on PLA, PLA/BPMS and PLA/BIOS blends. The samples were preliminarily

heated to 200°C to remove the thermal history and then, cooled at a rate of 10°C/min. During the cooling scans, none of the samples exhibited crystallization peak (T_{\cdot}) . This usually occurs because PLA crystallization is too slow to develop significant crystallinity. Several reviews have reported the low crystallization kinetics of PLA [41-43]. The second heating thermograms for the as received and processed PLA are shown in Figure 1. In both thermograms, an endothermic peak approximately at 60°C (representing excess enthalpy relaxation) is shown as the (T). For unprocessed neat PLA, a small peak at 170°C is observed and related to melting temperature with an enthalpy of 15.5 J g¹, while the cold crystallization peak could not be clearly observed. This might be because the unprocessed PLA does not have the ability to complete the crystallization process at the heating stage. The processed neat PLA exhibits a melting sharp peak at approximately 168°C and a defined cold crystallization peak at 100°C. In addition, the crystallinity of the processed PLA $(X_c=28\%)$ suggested that it increases during the extrusion when compared with unprocessed PLA ($X_{c}=16\%$). The second heating thermogram for the PLA/BPMS and PLA/BIOS blends are shown in Figure 2, where only one $T_{\rm s}$ can be observed, suggesting the complete miscibility of the melt strength enhancer additive (either BPMS or BIOS) with PLA. Moreover, the PLA blends exhibited a similar thermal behavior regarding the T_{σ} compared to the PLA without additive. The melting temperature of PLA/BPMS blends shifts to a lower temperature compared with the processed PLA. Double melting peaks appeared at about 163°C and 169°C in the PLA/BIOS blends and at 158°C and

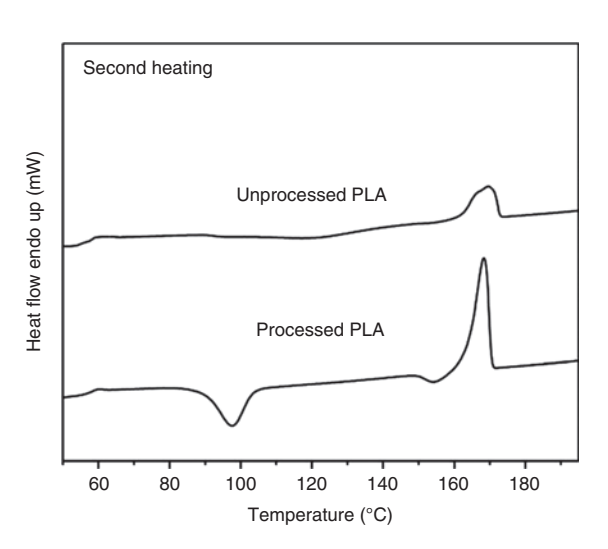


Figure 1: Differential scanning calorimetry (DSC) thermograms recorded during the second heating at the rate of 10°C/min for unprocessed and processed polylactide (PLA).

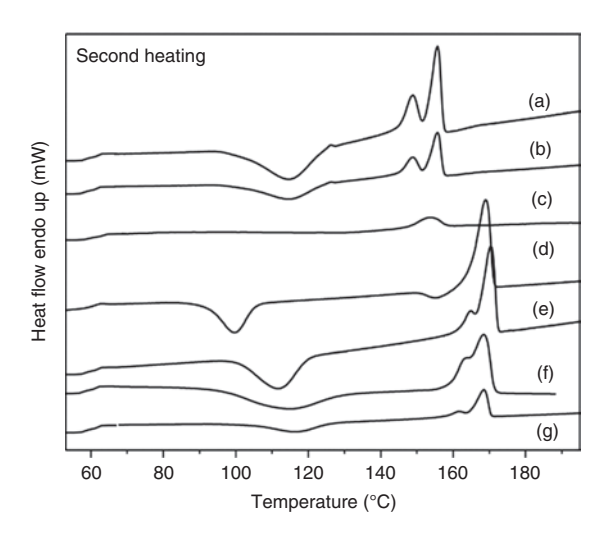


Figure 2: Differential scanning calorimetry (DSC) thermograms during the second heating at 10°C/min for: (a) PLA/BPMS-2, (b) PLA/BPMS-5, (c) PLA/BPMS-10, (d) processed PLA, (e) PLA/ BIOS-2, (f) PLA/BIOS-5 and (g) PLA/BIOS-10.

155°C in the PLA/BPMS blends. This behavior has been reported as a result of a lamellar rearrangement during crystallization of PLA [44]. The peak at the lower temperature is related to the melting of the disordered α ' crystalline form, which can be produced by annealing at lower temperatures, and its recrystallization into the ordered α form, while the second peak corresponds to the melting of the crystal α form [44–46]. Cartier et al. [47] described the double melting peaks as a result of the difference of crystalline structure that can exist in PLA. The cold crystallization onset of the PLA blends shifts to higher temperatures, around 15°C, and enlarged the peak width as the mass fraction of BPMS or the BIOS additives increase. The increase of the cold crystallization temperature indicates that the crystallization has become more difficult [41]. Even for the blends containing the higher additive content (10 wt%), the cold crystallization peak was no longer visible, especially for the PLA/BPMS-10 sample. Since the crystallization is a process associated with partial alignment of the molecular chains, this behavior could be attributed to the entanglement between the additive chains with the PLA that reduce its chain mobility, so PLA chains did not have enough time to reorganize into stable crystals. The crystallinity (X_n) of the samples was calculated using Eq. (1). The PLA is expected to crystallize up to a maximum level of 40-45% which corresponds to 37-42 J/g endothermic peaks (using 93 J/g as the theoretical value for the heat of fusion of PLA crystals [48]). The values observed for all samples including the T_o , melting temperature (T_m) , cold crystallization temperature (T_c) , melting enthalpy (ΔH_{∞}) , cold crystallization enthalpy (ΔH_{∞}) and associated degree of crystallinity (X) are presented in Table 4. As shown in this table, the percent of crystallinity decreased with an increase of the BPMS or BIOS additives. The PLA blends showed between 6% and 28% for the different melt strength enhancer contents examined. These results seem to indicate that the addition of the melt-strength enhancer diminishes the segmental movement of the PLA molecular chain changing its melting temperature and decreasing its ability to crystallize and/or recrystallize during processing.

3.2 Rheological properties

Dynamic rheological experiments were carried out at 180°C for the unprocessed and processed neat PLA, and the PLA/BIOS and PLA/BPMS blends. The viscoelastic properties were studied by measuring the storage modulus (*G'*), loss modulus (*G''*) and complex viscosity (η^*) within the linear viscoelastic region (10% strain). The end of the linear viscoelastic region is indicated by a decrease of G'value because G' is the parameter which is most sensitive to changes in microstructure.

As shown in Figure 3, the complex viscosity of the samples decreases with increasing shear strain rate, acting as a pseudoplastic fluid. The unprocessed PLA exhibits a clear Newtonian Plateau at low frequencies with a zero-shear viscosity (η_0) from around 2200 Pa·s and a shear thinning behavior at high oscillation frequency. The zero-shear viscosity was estimated from the Carreau model using the Rheoplus/32 V2.81 software as the viscosity value at very low shear rates or frequency

Table 4: Effect of melt strengthening additive on thermal properties of polylactide (PLA) determined by differential scanning calorimetry (DSC) (second heating at 10°C min-1).

Sample		T _{cc}	∆ H _{cc}	<i>T_m</i> (°C)		∆ H _m	X _c
		(°C)	C) (J g ⁻¹)	1	2	(J g ⁻¹)	(%)
Unprocessed PLA	60	_	_	_	170	15.5	16.6
Processed PLA	60	100	16	-	168	42.7	28.5
PLA/BPMS-2	60	114	29.8	148	155	49.3	21.4
PLA/BPMS-5	60	114	13.2	148	155	30.2	19.1
PLA/BPMS-10	60	-	-	-	153	5.1	6.1
PLA/BIOS-2	60	111	29.1	164	170	45.3	17.7
PLA/BIOS-5	60	114	16.6	163	169	30.5	15.6
PLA/BIOS-10	60	116	2.7	162	168	9.8	8.4

 ΔH_{co} , enthalpy of cold crystallization; ΔH_{m} , enthalpy of fusion; T_{c} , cold crystallization temperature; T_{c} , glass transition temperature; T_m , melting temperature; X_m , degree of crystallinity.

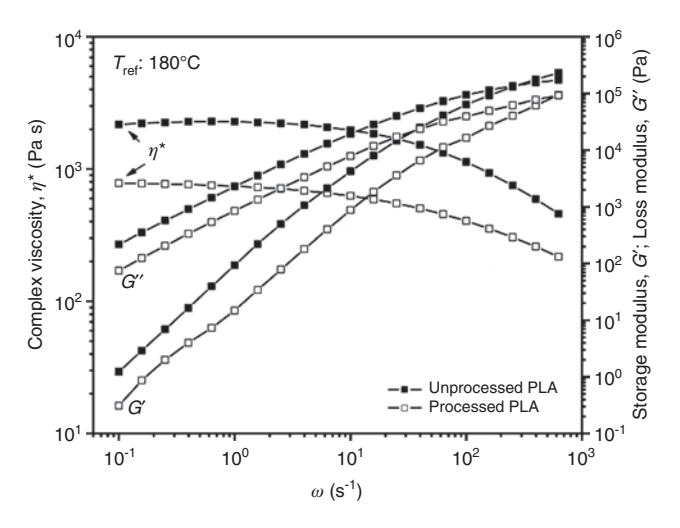


Figure 3: The viscoelastic properties: complex viscosity (η^*) , storage modulus (G') and loss modulus (G'') vs. angular frequency (ω) for unprocessed and processed polylactide (PLA).

approaching zero value (see Table 5). The processed neat PLA also exhibits a plateau region at low frequencies but with a lower zero-shear viscosity value compared with the unprocessed PLA (around 700 Pa·s). This could be attributed to degradation that suffers the PLA during its processing. Thermal degradation involves shortening molecular chains and therefore molecular weight loss leading to lower viscosities [49]. The characteristic relaxation time $(\tau_{...})$ was calculated by taking the inverse of the crossover frequency defined as the frequency where G' and *G*" are equal (Table 5). The relaxation time is important because it provides a time scale that indicates how long is required to relax after a deformation or stress is applied [50]. Accordingly, the characteristic relaxation time, crossover frequency and zero shear viscosity are important viscoelastic properties of the polymer related to the degree of entanglement. A higher crossover frequency indicates lower entanglements among the molecules and a lower characteristic relaxation time [51].

The curves of complex viscosity of PLA/BIOS and PLA/BPMS blends at various mass fractions of additive are presented in Figure 4. At low frequencies, PLA blends exhibit an indefinite plateau region, while the zero-shear viscosity values increase with increasing additive content. This enhancement of viscosity is due to greater entanglements between chains by adding higher quantity of melt strength enhancer additive, forming a network in which more PLA chains are anchored. This leads to reduced segmental mobility of PLA chains at low shear rates. At higher frequencies, PLA/BIOS and PLA/BPMS blends exhibit a shear thinning behavior where the complex viscosity decreases with increasing shear rate due to the PLA chains which are disentangled. It can be noted that the PLA blends containing BIOS additive exhibit higher viscosities.

The corresponding storage modulus (G') and loss modulus (G'') are shown in Figures 5 and 6 for PLA/BPMS

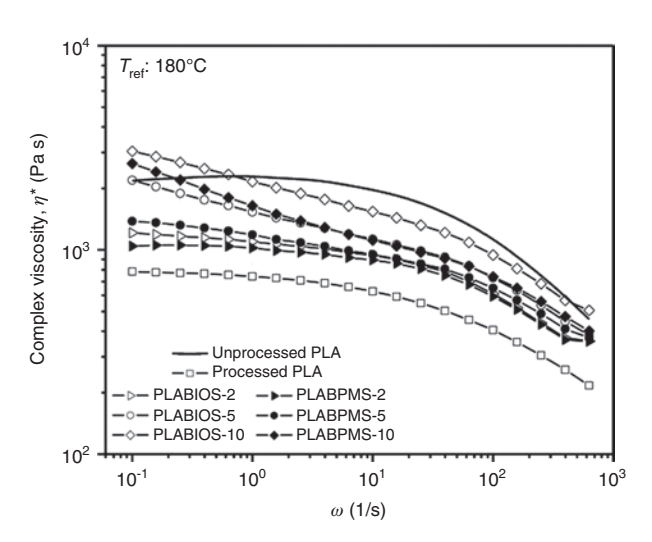


Figure 4: Dynamic viscosity (η^*) vs. angular frequency (ω) for PLA/BPMS and PLA/BIOS blends with varying contents of melt strength enhancer additive either Paraloid BPMS-250 or Biostrength 700.

Table 5: Rheological parameters for unprocessed polylactide (PLA) and PLA/BIOS and PLA/BPMS blends.

Sample	$\eta_{_0}$	G_N^o	M_{e}	τ"	MFl	MS
	(Pa·s)	(10 ⁵ Pa)	(10 ⁴ g/mol)	(s)	(g/10 min)	(%)
Unprocessed PLA	2283	0.97	3.7	0.004	8.7	-1
Processed PLA	728	0.95	4.4	0.0016	25.4	-48
PLA/BPMS-2	984	1.33	3.2	0.003	24.7	58
PLA/BPMS-5	1094	1.48	2.8	0.003	21.6	70
PLA/BPMS-10	1280	1.71	2.4	0.003	16.4	70
PLA/BIOS-2	1076	1.41	3.0	0.003	20.7	64
PLA/BIOS-5	1263	1.69	2.5	0.003	15.4	81
PLA/BIOS-10	1632	1.82	2.3	0.003	15.6	87

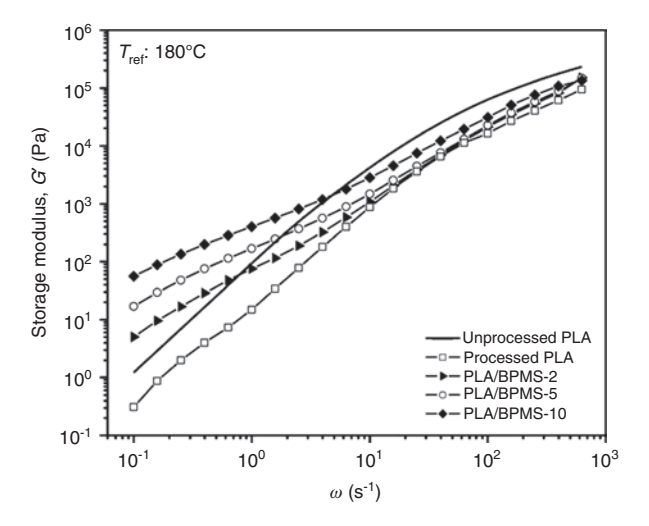


Figure 5: Storage modulus (G') vs. angular frequency (ω) for PLA/ BPMS blends with varying contents of Paraloid BPMS-250 melt strength enhancer.

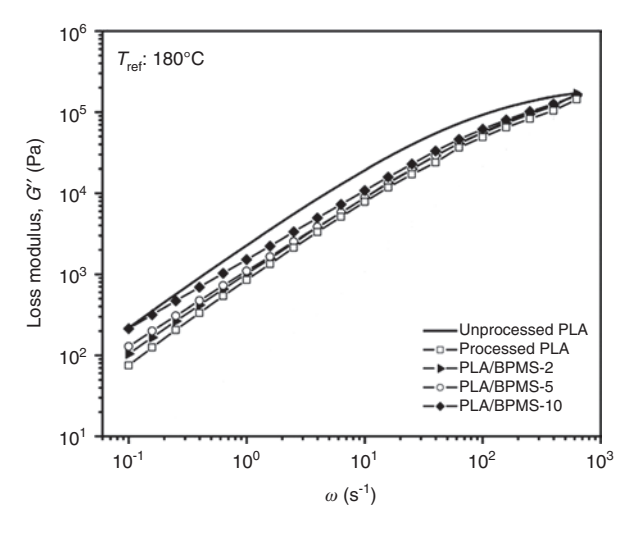


Figure 6: Loss modulus (G'') vs. angular frequency (ω) for PLA/ BPMS blends with varying contents of Paraloid BPMS-250 melt strength enhancer.

and Figures 7 and 8 for PLA/BIOS blends, respectively. At low frequencies, PLA blends also exhibit the rheological behavior characterized by a storage modulus G' smaller than the loss modulus G''. The dynamic loss modulus G" of PLA blends indicates that the blends with higher additive content have slightly higher G' values than that of the processed PLA at low frequencies. This is because the addition of additive produced a material with more energy dissipation. At high frequencies, *G*" becomes more insensitive to the network structure. At low frequencies, the storage modulus G' increases with increasing additive content and PLA/BIOS blends exhibit the highest values,

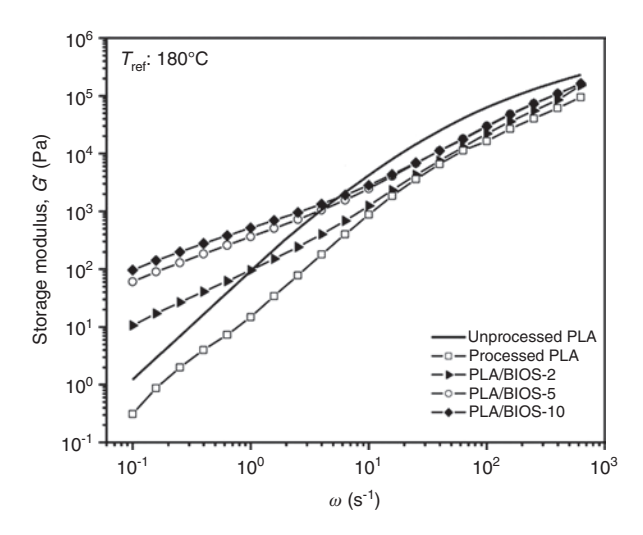


Figure 7: Storage modulus (G') vs. angular frequency (ω) for PLA/ BIOS blends with varying contents of Biostrength 700 melt strength enhancer.

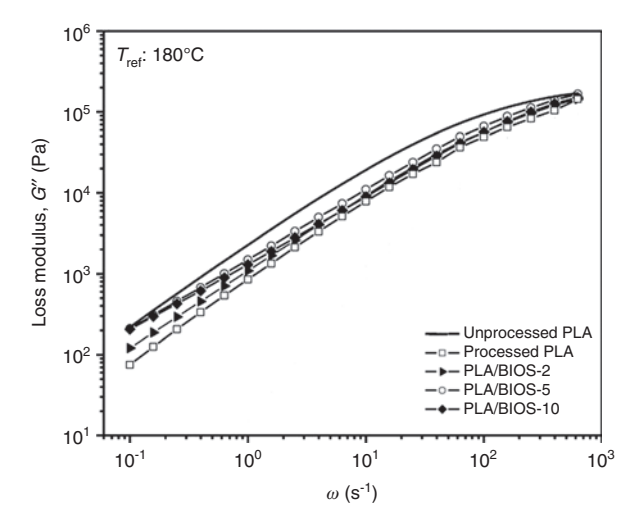


Figure 8: Loss modulus (G'') vs. angular frequency (ω) for PLA/ BIOS blends with varying contents of Biostrength 700 melt strength enhancer.

i.e., PLA/BIOS-10 has a storage modulus from around 100 Pa while processed PLA presents a value from around 0.5 Pa. This could be explained by the entanglements of PLA chains with the long additive chains creating a physical network where each chain is connected to all others by a sequence of knots to form a single macroscopic entity with higher melt elasticity. The melt strength is related to the elongational viscosity of the polymer, η_F , that is normally measured in a tensile test using an extensional rheometer. However, the difficulties encountered in using this type of rheometer led the researches to develop alternative experimental techniques [52]. In this work, the elongational

viscosity of the unprocessed PLA and the PLA/BIOS and PLA/BPMS blends was determined from the Cogswell converging flow model [38]. The elongational viscosities as a function of elongation rate after Bagley correction for PLA/BIOS and PLA/BPMS blends are shown in Figures 9 and 10, respectively. The experiments were carried out by a screw-extrusion capillary rheometer. The elongational viscosity increased with the additive content (Paraloid BPMS-250 or Biostrength 700) as a result of greater entanglements between chains which leads to a high resistance to break in the melt during stretching. PLA/BIOS blends exhibited slightly greater results in comparison with PLA/ BPMS blends, which could be because they have longer and heavier chains creating more entanglements, thus giving rise to a higher viscosity. So, the increase in elongation viscosity confirms the melt strengthening properties of PLA with the additive. An increase of the elongational properties also means a higher melt elasticity of entangled PLA compared with the unprocessed polymer. Figure 11 qualitatively illustrates the effect of addition of BIOS and BPMS melt strengthener additives to the PLA melt. The PLA melts encompassing additives are remarkably unbending and hold their shape better than the neat PLA. Usually, when a polymer increases its elongational viscosity, it exhibits strain hardening. Strain hardening has a positive effect on the sample deformation. When a strain hardening material is stretched, an inhomogeneity occurring somewhere in the sample will disappear as the larger elongation of the thinner cross section area leads to a higher elongational viscosity. Contrarily, for a nonstrain hardening material, the sample will finally break by

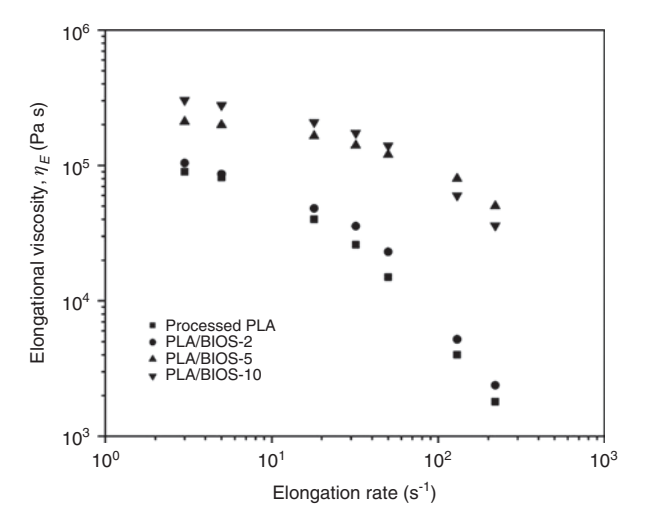


Figure 9: Elongational viscosity as a function of elongational rate for polylactide (PLA) and PLA/Biostrength (BIOS) blends with varying contents of Biostrength 700 melt strength enhancer.

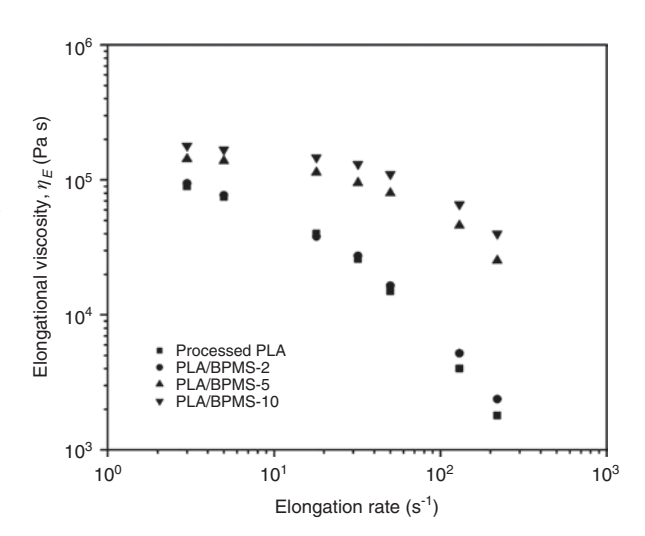


Figure 10: Elongational viscosity as a function of elongational rate for polylactide (PLA) and PLA/BPMS blends with varying contents of Paraloid BPMS-250 melt strength enhancer.

stretching [53]. Palade et al. [49] studied the elongational viscosity vs. time for PLA samples with different nominal L:D values at a rate of $\dot{\varepsilon}$ =0.1 s^{-1} . The most notable feature was a strong strain hardening behavior (the extensional viscosity increased by two orders of magnitude). When the PLA is melt blended with a melt strength enhancer additive, the molecular chains of PLA and those of the high molecular weight acrylic copolymer are intertwined or connected to one another physically, forming knots or links, forming chain entanglements. The entanglement concept is often discussed and revised in the literature, as it is one of the most typical features of polymer chains and a key factor controlling the melt rheology and the solid-state deformation mechanisms [54]. Chain entanglements in a melt are essentially the physical interlocking of polymer chains, which is a direct consequence of chain overlapping. In a polymer melt, chain overlap, and hence the number of entanglements (or alternatively entanglement density), increases with polymer chain length or molecular weight [55]. An important parameter for entangled macromolecules is the average molecular weight spacing between entanglement junctions, i.e., the entanglement molecular weight, M_a , which can be calculated from plateau modulus rheology measurements through an equation derived from the theory of rubber elasticity:

$$M_e = \frac{\rho RT}{G_N^0} \tag{8}$$

where $\rho(Kg/m^3)$ is the density of the polymer at reference temperature T(K), R is the universal gas constant

 $R=8.314(\text{kPa}\cdot\text{m}^3)/(\text{kmol}\cdot\text{K})$ and $G_N^0(\text{kPa})$ is the plateau modulus. This equation is based on the assumption that the entanglement points behave like cross-links in the classical rubber-elasticity theory. The rubber plateau modulus (G_{ν}^{0}) is defined as the "most elastic" dynamic modulus found at the minimum of $tan(\delta)$. Upon further heating, the polymer starts to disentangle and the dynamic modulus decays further out of the measurable range. In this temperature range, the onset of a second "viscous" peak is observed in $tan(\delta)$, which indicates that the material becomes liquid-like.

In this work, estimations of the molecular weight between entanglements M_{ρ} in the PLA melt were made. Accordingly, the plateau modulus G_N^0 of the unprocessed PLA, the PLA/BIOS and the PLA/BPMS blends was obtained from the dynamic data as the storage modulus G' in the plateau zone at the frequency where $tan(\delta)$ was at a minimum. It was calculated using the Rheoplus/32 V2.81 software. For unprocessed PLA, an M_a of 3.7×10^4 was obtained and PLA blends were also calculated, as shown in Table 5. The values of M_a indicated that the occurrences of chain entanglements were obtained in PLA/BIOS and PLA/BPMS blends but there was insignificant entanglement in neat PLA. It can be seen that the values of M of the PLA/BPMS blends are higher than that of the PLA/BIOS blends, indicating that the segment packing in the PLA/BPMS blends is in a looser state and the entanglement density is lower. The inter- and intrachain entanglements of the PLA/BPMS blends are less than those of the PLA/BIOS blends. The entanglements molecular weight, M_{o} , of the PLA blends was decreased by increasing the weight percentage of additive added to PLA. So, the chain entanglements were improved and the entanglement density was decreased. In addition, the relaxation time τ , obtained with the inverse of crossover frequency (where G'=G''), was obtained. The relaxation time τ of the PLA/BPMS blends is shorter than that of the PLA/BIOS blends, suggesting less entanglements and stronger mobility of the chain segments in the PLA/BPMS blends. In this work, melt strength has been assessed by measuring the vertical length of PLA and PLA blends extrudates after a certain amount of time. Shorter lengths indicate better melt strength and, consequently, less sag [39]. Melt strength was determined by a screw-extrusion capillary rheometer and was calculated as the ratio of the diameter of the capillary (0.2 cm) to the diameter of the 15 cm long polymer extrudate at a distance of 7 cm above the end of the extrudate. Unprocessed PLA does not exhibit good melt strength (Table 5), whereas for the processed PLA, it was impossible to obtain an extrudate with the necessary length. PLA/

BIOS and PLA/BPMS blends have significantly improved melt strength, as compared with unprocessed PLA. It can also be seen that the PLA blends exhibit improved melt strength with increasing concentrations of any additive. The determination of the negative melt strength ratio for unprocessed PLA indicates that the extrudate has a smaller diameter than the capillary diameter at the point measured. By contrast, the positive ratios for PLA blends indicate that the measured extrudate diameter was larger than the capillary one.

3.3 Blend morphology

The SEM micrographs of the PLA/BIOS and PLA/BPMS blends fracture surfaces are shown in Figure 12. Miscible blends are usually homogeneous and transparent, so we can see that both acrylic additives are homogenously dispersed in a continuous PLA phase. The fracture surface of neat PLA (Figure 12A) appeared relatively smooth, indicating a typical brittle fracture with no appreciable plastic deformation and a rapid propagation of the crack. In Figure 12B and C, it can be seen that the incorporation of 2 wt% of additives does not change the fracture mode of the blend compared with the neat PLA. By contrast, with 5 wt% and 10 wt% of acrylic additives, the mode of fracture of PLA blends changes to a more ductile one, indicating that both BIOS and BPMS additives acting like a PLA plasticizer, as can be seen in Figure 12D-G where rough and plastic deformation can be observed.

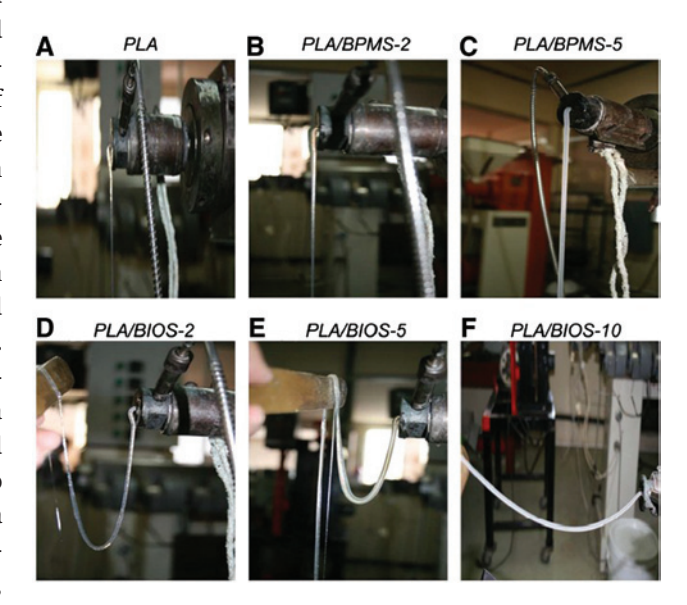
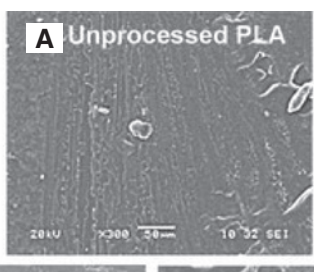


Figure 11: Examples to illustrate the melt strengthening of polylactide (PLA) by adding an acrylic copolymer during melt processing.



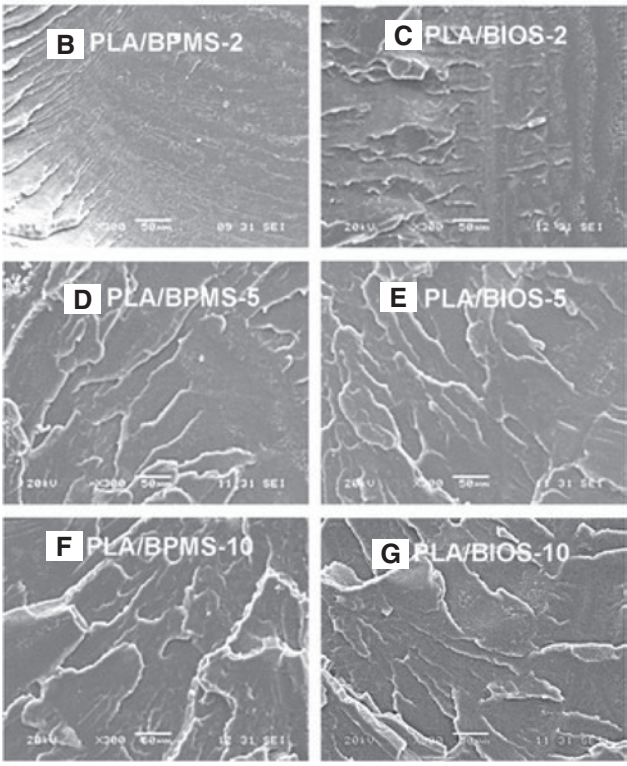


Figure 12: Scanning electron microscopy (SEM) micrographs (A–G) of fractured surfaces of polylactide (PLA) and PLA blends with varying contents of melt strength enhancer additive either Paraloid BPMS-250 or Biostrength 700.

4 Conclusions

In order to find out the effect of two commercial melt strength enhancer additives on the thermal, rheological and morphological properties of PLA, different blends of PLA/additive were melt-blended using a screw extruder. Thermal analyses results showed the complete miscibility of the melt strength enhancer additive (either BPMS or BIOS) with PLA resin, since only one T_g was observed for all blends. The cold crystallization onset of the PLA blends shifts to higher temperatures and their crystallinity decreased with an increase of the BPMS or BIOS additives compared to neat PLA. This behavior indicates a lower crystallization capability of PLA in the blends, i.e., the addition of the melt-strength enhancer decreases the ability of PLA

to crystallize and/or recrystallize during processing. The rheological tests indicated that zero-shear viscosity and storage modulus of the PLA/BPMS and PLA/BIOS blends were significantly increased with the additive content. The entanglement molecular weights (M₂) of PLA/BPMS and PLA/BIOS blends were lower than those of unprocessed and processed neat PLA (*M*_o≈4×10⁴ g/mol), which suggests greater chain entanglements and a higher entanglement density (ν_a). The relaxation time τ of the PLA/BPMS blends is shorter than that of the PLA/BIOS blends, suggesting less entanglements and stronger mobility of the chain segments in the PLA/BPMS blends. The elongational viscosity and the melt strength of the blends increased with the additive content (Paraloid or BIOS). These findings suggest the entanglements of PLA chains with those of the high molecular weight additive, creating a physical network which reduces the segmental mobility of PLA and leads to a high resistance to break in the melt during stretching.

The analysis of SEM micrographs seems to confirm the miscibility of the acrylic additives with the PLA and suggests that they plasticize the PLA at 5% and 10% w/w content.

Acknowledgments: The authors would like to thank Ms. I.Q. Silvia Beatriz Andrade Canto for the SEM micrographs and Ms. M. en C. Maria Veronica Moreno Chulim for assistance with DSC characterization.

References

- [1] Vroman I, Tighzert L. Mater. 2009, 2, 307-344.
- [2] Vink ETH, Rábago KR, Glassner DA, Gruber PR. *Polym. Degrad. Stab.* 2003, 80, 403–419.
- [3] Yoon CS, Ji DS. Fibers Polym. 2003, 4, 59-65.
- [4] Dorgan JR, Lehermeier H, Mang M. J. Polym. Environ. 2000, 8, 1-9.
- [5] Lim LT, Auras R, Rubino M. Prog. Polym. Sci. 2008, 33, 820–852.
- [6] Avérous L. In Monomers, Polymers and Composites from Renewable Resources, 1st ed., Belgacem MN, Gandini A, Eds., Elsevier: Amsterdam, 2008, Chap. 21, p. 433.
- [7] Auras R, Lim LT, Selke SEM, Tsuji H, Eds., Poly(lactic acid) Synthesis, Structures, Properties, Processing, and Application, 1st ed., John Wiley & Sons: New Jersey, 2010.
- [8] Garlotta D. J. Polym. Environ. 2001, 9, 63-84.
- [9] Henton DE, Gruber P, Lunt J, Randall J. In Natural Fibers, Biopolymers, and Biocomposites, 1st ed., Mohanty AK, Misra M, Drzal LT, Eds., CRC Press Taylor & Francis: Florida, 2005, Chap. 16, p. 527.
- [10] Gupta MC, Deshmukh VG. Colloid Polym. Sci. 1982, 260, 514–517.
- [11] Zhang X, Espiritu M, Bilyk A, Kurniawan L. *Polym. Degrad. Stab.* 2008, 93, 1964–1970.

- [12] Muke S, Ivanov I, Kao N, Bhattacharya S. Polym. Int. 2001, 50,
- [13] Lau HC, Bhattacharya SN, Field GJ. Polym. Eng. Sci. 1998, 38, 1915-1923.
- [14] Dean KM, Petinakis E, Meure S, Yu L, Chryss A. J. Polym. Environ. 2012, 20, 741-747.
- [15] Frankland J. What about Melt Strength?, Issue June 2013. Available at http://www.ptonline.com/columns/what-about-meltstrength. Retrieved: February 2015.
- [16] Liu W, Li H, Wang X, Du Z, Zhang C. Cell. Polym. 2013, 32, 343-365.
- [17] Södergard A, Stolt M. Prog. Polym. Sci. 2002, 27, 1123-1163.
- [18] Carlson D, Nie L, Narayan R, Dubois P. J. Appl. Polym. Sci. 1999, 72. 477-485.
- [19] Carlson D, Dubois P, Nie L, Narayan R. Polym. Eng. Sci. 1998, 38, 311-321,
- [20] Zhou ZF, Huang GQ, Xu WB, Ren FM. Express Polym. Lett. 2007, 1, 734-739.
- [21] Najafi N, Heuzey MC, Carreau PJ. Polym. Eng. Sci. 2013, 53,
- [22] Corre YM, Duchet J, Reignier J, Maazouz A. Rheol. Acta 2011, 50, 613-629.
- [23] Mihai M, Huneault MA, Favis BD. Polym. Eng. Sci. 2010, 50, 629-642.
- [24] Pilla S, Kim SG, Auer GK, Gong SQ, Park CB. Polym. Eng. Sci. 2009, 49, 1653-1660.
- [25] Han T, Xin Z, Shi Y, Zhao S, Meng X, Xu H, Zhou S. J. Appl. Polym. Sci. 2015, 132, 41977-41987.
- [26] Rasal RM, Janorkar AV, Hirt DE. Prog. Polym. Sci. 2010, 35, 338-356.
- [27] Ge XG, George S, Law S, Sain M. J. Macromol. Sci., Part B: Phys. 2011, 50, 2070-2083.
- [28] Taib RM, Ghaleb ZA, Mohd Ishak ZA. J. Appl. Polym. Sci. 2012, 123, 2715-2725.
- [29] Zhang H, Liang H, Bian J, Hao Y, Han L, Wang X, Zhang G, Liu S, Dong L. Polym. Int. 2013. doi: 10.1002/pi. 4615.
- [30] Yuqiong X, Min Y, Jinping Q. Wuhan Univ. J. Nat. Sci. 2009, 14, 349-354.
- [31] Enhancing Biopolymers: Additives Are Needed for Toughness, Heat Resistance and Processability. Available at http://www. mmsonline.com/articles. Retrieved February 2015.
- [32] ©Rhom and Haas. Paraloid™BPMS-250 Melt Strength Enhancer for Polylactic Acid 2008. http://www.dow.com/assets/attachments/business/pbm/paraloid_bpms/paraloid_bpms_250/ paraloid_bpms-250.pdf. Retrieved February 2015.
- [33] NatureWorks LLC. Ingeo™ Biopolymer 4032D Technical Data Sheet 2011. http://www.natureworksllc.com/~/ media/Technical_Resources/Technical_Data_Sheets/

- TechnicalDataSheet_4032D_films_pdf. Retrieved February
- [34] ©Arkema Inc.Biostrength® 700 Melt Strength Enhancer 2013. http://www.additivesarkema.com/export/sites/acrylicmodifiers/.content/medias/downloads/literature/biostrength-700-pa.pdf. Retrieved February 2015.
- [35] Brake J, Seshadri SR. US Patent WO2007089451A2; Aug. 9,
- [36] O'Connor A, Riga A, Turner II JF. J. Therm. Anal. Calorim. 2004, 76, 455-470.
- [37] ASTM Standard D1238-13, Test Method for Melt Flow Rates of Thermoplastics by Extrusion Plastometer. American Society for Testing and Materials.
- [38] Cogswell FN. Polym. Eng. Sci. 1972, 12, 64-73.
- [39] ASTM Standard D5422-09, Test Method for Measurement of Properties of Thermoplastic Materials by Screw-Extrusion Capillary Rheometer. American Society for Testing and Materials.
- [40] Morris JC, Bradley JR, Seo KS. US Patent, 5, 989, 663; Nov. 23,
- [41] Yeh JT, Tsou CH, Huang CY, Chen KN, Wu CS, Chai WL. J. Appl. Polym. Sci. 2010, 116, 680-687.
- [42] Santis FD, Pantani R, Titomanlio G. Thermochim. Acta 2011, 522, 128-134.
- [43] Saeidlou S, Huneault MA, Li H, Park CB. Prog. Polym. Sci. 2012, 37, 1657-1677.
- [44] Nijenhuis AJ, Colstee E, Grijpma DW, Pennings AJ. Polym. 1996, 37, 5849-5857.
- [45] Tábi T, Sajó IE, Szabó F, Luyt AS, Kovács JG. Express Polym. Lett. 2010, 4, 659-668.
- [46] Pan P, Zhu B, Kai W, Dong T, Inoue Y. Macromol. 2008, 41, 4296-4304.
- [47] Cartier L, Okihara T, Ikada Y, Tsuji H, Puiggali J, Lotz B. Polym. 2000, 41, 8909-8919.
- [48] Fisher EW, Stergel HJ, Wegner G. Kolloid ZZ Polym. 1973, 251, 980-990.
- [49] Paladel-I, Lehermeier HJ, Dorgan JR. Macromol. 2001, 34, 1384-1390.
- [50] Morrison FA. Understanding Rheology, Oxford University Press: New York, 2001.
- [51] Larson RG. The Structure and Rheology of complex Fluids, Oxford University Press: New York, 1999.
- [52] Baldi F, Franceschini A, Riccò T. Rheol. Acta 2007, 46, 965-978.
- [53] Münstedt H, Kurzbeck S, Stange J. Polym. Eng. Sci. 2006, 46, 1190-1195.
- [54] Lomellini P. Polym. 1992, 33, 1255-1260.
- [55] Shenoy SL, Bates WD, Frisch HL, Wnek GE. Polym. 2005, 46, 3372-3384.